Green Chemistry

Economic and environmental potentials for natural gas to enhance biomass-to-liquid fuels technologies

Yanan Zhang, Asad H. Sahir, Eric C. D. Tan, [ID] Michael S. Talmadge, Ryan Davis, Mary J. Biddy and Ling Tao [ID] *

With the increased availability of low-cost natural gas (NG), co-conversion of natural gas and biomass-to-liquid (GBtL) fuels has gained interest from industry and the U.S. Department of Energy due to the potential to improve liquid fuel yields while lowering greenhouse gas (GHG) emissions. In this article, we explore the conceptual process design and cost comparison of liquid biofuels using both biomass-derived gas intermediates and natural gas, as well as studies on quantification and assessment of sustainability metrics including life cycle/GHG emissions. Additionally, we have performed sensitivity analysis to understand the impact from variations of the biomass-to-NG ratio, design assumptions, and NG prices on process economics. This is to understand key cost drivers, parameters influencing the environment, and to discover opportunities to optimize the use of NG along with biomass. Our analysis shows that different blending ratios of natural gas/biomass have a large effect on the economic and environmental performance of the GBtL fuels. Co-processing NG enables the economic feasibility of converting biomass to the liquid fuel but at the expense of environmental sustainability. This study determined that the maximum amount of NG that can be blended with biomass would be 28% to meet the Renewable Fuel Standard (RFS) GHG emission targets for advanced fuels, with a resulting minimum fuel selling price (MFSP) of $2.75 per gallon gasoline equivalent (GGE). In addition, the paper demonstrates the impact of the co-conversion operation on equipment design, raw materials, utility consumption, and overall process economic performance for the GBtL system. A secondary outcome: This study shows that renewable liquid fuel could be cost competitive with fossil-derived liquid fuel if further improvements and optimizations could be made to blending ratios of NG, optimization of heat integration of the process, and reduction of excess hydrogen and excess electricity production.

1. Introduction

According to recent U.S. Energy Information Administration (EIA) projections, the consumption of world petroleum and other liquid fuels will increase by 38% by 2040 from 2014, and the transportation and industrial sectors will account for 92% of the global liquid fuel demand in 2040.[1] This growing demand encourages the exploration of a variety of feedstocks for transportation fuels production with biomass being the only renewable energy source[2] that has the capability to present a viable substitute for petroleum-based liquid transportation fuels.[3]

Literature has detailed the process configurations for biomass-to-liquid (BtL),[4] coal-to-liquid (CtL), and gas-to-liquid

(GtL).[5–7] In the case of BtL and CtL, a gasification reactor is employed that converts the carbonaceous feedstock into syngas. The syngas is subsequently converted to hydrocarbon liquids through the Fischer–Tropsch (FT) process. The advantage of the FT process is that it can produce hydrocarbons of varying length from any carbonaceous feedstock (*e.g.*, coal, NG, or biomass), provided that the desired H_2/CO ratio is attained. The production of hydrocarbon liquids from FT synthesis using cobalt-based catalysts requires an optimum H_2/CO ratio in the range of 2.0–2.2.[8]

The H_2/CO ratio plays an essential role in the FT process. In the case of biomass and coal gasification, the H_2/CO ratio of the effluent syngas is adjusted *via* water–gas shift reaction followed with a subsequent CO_2 removal step.[9,10] Cobalt-based catalysts have a low water gas shift activity, which implies that syngas should have a H_2/CO ratio of 2.15 to ensure a high conversion.[11] In comparison, iron-based catalysts possess a higher water–gas shift reaction activity.

National Renewable Energy Laboratory, 15013 Denver West Parkway, Golden, CO 80401, USA. E-mail: Ling.Tao@nrel.gov; Tel: +1-303-384-7809

Supported cobalt catalysts are preferred for the FT synthesis (FTS) step in the GtL process owing to its high activity and selectivity to linear paraffins.[12] For instance, supported cobalt-based catalysts were employed in Shell's Middle Distillate Synthesis process at Bintulu, Malaysia, a GtL plant with a 14 700 barrels per day capacity using fixed bed reactors, and was used in Shell's Pearl project in Qatar.[12,13]

The recent interest in co-conversion of natural gas and biomass-to-liquid (GBtL) makes it imperative to understand the optimization and integration of natural gas (NG) and biomass into a hydrocarbon liquid fuel conversion process. Recent studies have shown the possibility of reforming NG and biomass-derived synthesis gas (syngas) in a single reactor; this offers research and development (R&D) opportunities for subsequent process intensification.[4]

The heating values of woody biomass, NG, and FT products are listed in Table 1. With a relatively high NG heating value, the liquid fuel yield would be enhanced when biomass is blended with NG. Process synthesis and optimization studies related to BtL,[14,15] CtL,[16] hybrid biomass and coal,[17,18] and hybrid biomass and NG processes[19] have been recently reported.[19–22] Process strategies associated with co-conversion of NG with biomass have drawn interest due to the current lower cost of NG relative to biomass, and for its potential for lower GHG emissions relative to petroleum.[23] The methane-rich composition of NG offers a high hydrogen-to-carbon ratio, which could potentially increase the overall carbon yield in liquid products and reduce the quantity of CO_2 produced.[14] Process concepts on co-conversion of biomass and NG have been proposed previously for production of methanol with reduced CO_2 emissions (Hynol process)[24] and for generating hydrogen and methanol for fuel cell vehicles.[25]

The GtL process provides an effective mechanism in increasing the supply of domestic transportation fuels by reducing dependence on oil imports, thus enhancing energy security.[6] Studies have shown that the GtL process exhibits carbon conversion efficiency (i.e., carbon in the feedstock that is converted to fuels) as high as 52%,[26] which is significantly higher than those from CtL (28%–34%[27]) and BtL (43%[28]), as shown in Table 1. In addition to high carbon efficiency from GtL, significant drivers for the development of the GtL technology could be attributed to the following factors:[29]

• The GtL process has high exothermicity, where the excess heat generated could be configured to produce electricity and steam.

• It enables the diversification of market risks by offering an opportunity to convert NG by providing an alternative option to liquefying NG.

• It offers an alternative to facilitate utilization of large quantities of gas associated with oil production on site, as well as applied at offshore gas fields.

• The global demand for diesel has the potential to increase from 25 million (MM) barrels per day in 2011 to 37 MM barrels per day by 2035.[30]

Another significant motivation for the development of technologies based on the GtL platform is its potential to utilize stranded reserves that are located more than 5000 km from consumption centers where traditional transport technologies could not be utilized, due to investment risks.[29] The stranded NG reserve is defined as NG discovered in conventional gas and oil fields that is not commercially producible and is estimated to be 2612 trillion cubic feet in the world (outside North America).[31]

Furthermore, another possibility envisioned for GtL technologies is the opportunity to monetize smaller volumes of gas (<25 MM standard cubic feet per day [scfpd] of gas), which may be applied in a cost-effective conversion of NG streams to valuable products. The small-scale GtL process provides an alternative opportunity when combined with biomass gasification, instead of being flared. Process synthesis and optimization studies would be needed to address the conversion of biomass and NG to transportation fuels.[32–34] An important focus in process design requires modularity, simplicity, automation, and robustness of operation,[35] especially for a wide spectrum of facility sizes.

The focus of this article is to assess the techno-economic analysis (TEA) of the co-conversion of biomass and NG (at various blending ratios) to transportation fuels. There are limited studies that focus on the TEA for GBtL. Chakravarti et al. modeled the NG-enhanced BtL process based on Praxair's patent.[36,37] In the Chakravarti study, an H_2-rich syngas stream is generated by a steam methane reformer (SMR), which is fed a combination of NG and tail gas generated in the FT synthesis section.[36] It was concluded that when producing gasoline, diesel, and kerosene in ratios commensurate with demands in the United States (U.S.), the overall cost of liquid fuel production ranges are: $109 per barrel (bbl)– $129 per bbl for a 1-thousand-barrels-per-day (kBD) plant, $85 per bbl–$106 per bbl for a 5-kBD plant, $75 per bbl–$95 per bbl for a 10-kBD plant, and $66 per bbl–$86 per bbl for a 50-kBD plant.[38] Onel et al. modified the process synthesis and a global optimization framework for the thermochemical conversion of biomass and GBtL to co-produce the liquid fuels and olefins.[39] It was observed that increasing the olefins production level significantly increases the profit of the refinery.[39]

Liu et al. developed two designs for coproduction of electricity and FT to liquid from a co-feed of NG and biomass, one with CO_2 venting (OT-V) and the other with CO_2 capture (OT-CCS) of 1.6 10^6 t CO_2 per year GBtL-OT-CCS.[40] In this study, the electricity price was reported at 98.9 and 135.7 $ per megawatt per hour if FT liquid fuels sold at $75 per bbl for

Table 1 Heating value of fuels and feedstocks

	Lower heating value (LHV) (BTU per lb)	H/C ratio	Carbon efficiency
Wood	6622	7.2–8.4	43%
NG	20 267	4.0	52%
Coal	9773 (wet basis)	1.0	28–34%
Naphtha	19 320	1.6–2.3	—
Diesel	18 397	—	—

GBtL-OT-V and GBtL-OT-CCS, respectively.[40] Wright *et al.* investigated the NG blending wall in biofuel production.[41] In this study, they showed that less than 19.1% of NG on an LHV energy basis (7.83 wt%) could be blended to avoid exceeding the emissions limits established by the Renewable Fuel Standard (RFS) 2.[41]

This GBtL TEA provides baseline cost results for hydrocarbon liquid fuel production, which can be viewed as a near-term deployment opportunity for renewable jet fuel production. Sensitivity analyses are performed to identify key cost drivers and guide future R&D, as well as near-term deployment strategies.

In addition to the economic feasibility, overarching concerns such as environmental sustainability also need to be addressed for sustainable biofuel production. In this study, life cycle assessment (LCA) is also performed in tandem with TEA to assess life cycle impacts associated with the production of hydrocarbon blendstock from biomass/NG co-processing *via* the FT process. The associated greenhouse gas and life cycle analyses are included to provide insight on the carbon footprint for liquid fuels production from the GBtL technology. LCA results provide a better understanding of the processes from the environmental aspects, and consequently, a more informed assessment and comparison of the technologies can be made.

2. Methods

2.1 General TEA methodology

Detailed TEA of co-conversion of NG and woody BtL fuels is performed at the plant scale of 50 MM gallon gasoline equi-

valent (GGE) hydrocarbon fuels production annually. The 2016 U.S. Billion-Ton Update estimates that by 2030 there will be enough agricultural and forest resources to sustainably provide at least one billion dry tons of biomass annually. While all biomass resources can be used as feedstocks for BtL processes, the scope of this study only focuses on woody biomass. The economic analysis includes a conceptual process design that leads to the development of a detailed process flow diagram (based on research or commercial data); rigorous material and energy balance calculations (*via* a commercial simulation tool, *i.e.*, Aspen Plus); capital and project cost estimations (*via* an in-house model using spreadsheets); a discounted cash flow economic model; and the calculation of a minimum fuel selling price (MFSP). The conceptual process design for the GBtL process is illustrated in Fig. 1. The baseline process model is based on previous National Renewable Energy Laboratory (NREL)-developed indirect gasification of biomass models,[42] BtL *via* FT technology models.[43]

The operating expense (OPEX) calculation for the designed facility is based on material and energy balance calculations using Aspen Plus process simulations.[44] All of the unit costs for materials are listed in Table 2 in 2011 U.S. dollars.

For coproduct yield of wax, we use an equivalent mass flow of wax based on low heating value, which means that the high molecular hydrocarbon mass flows from distillation columns were converted to the equivalent wax mass flow based on the low heating value of wax. The unit wax price is based on the equivalent wax mass flow.

All costs are adjusted to 2011 U.S. dollars using the Plant Cost Index from Chemical Engineering Magazine,[45] the
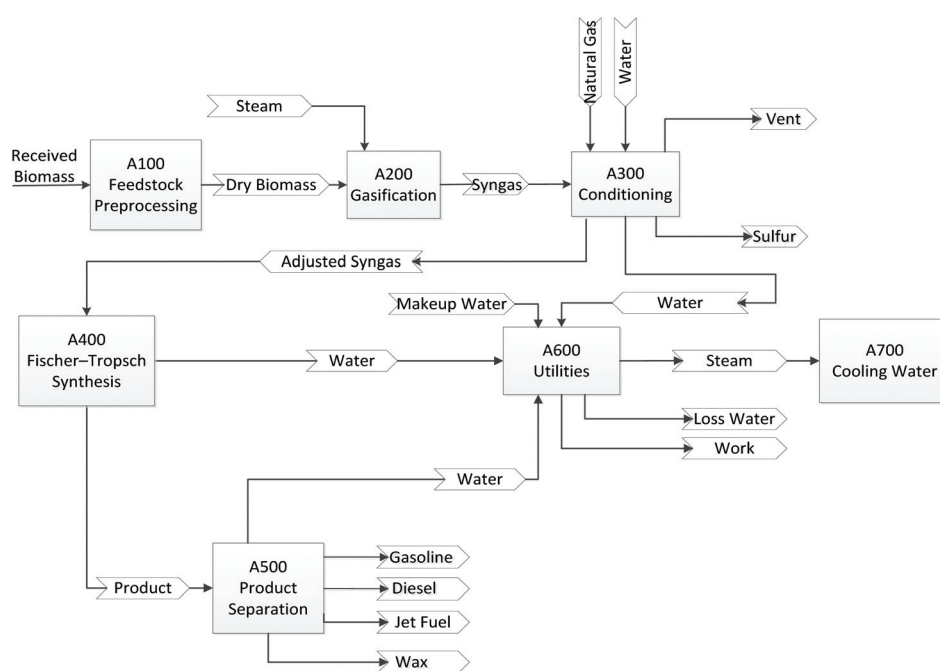

Fig. 1 Process flow diagram for the GBtL process. Note that all areas have either been commercialized or demonstrated at commercially relevant scales.

Table 2 Unit prices for raw materials and products (2011$)[42,43,48,51–59]

Materials	Cost
Woody biomass	$80 per ton
NG	$239 per ton ($5 per MMBTU)
Electricity	$0.0572 kWh
Magnesium oxide (MgO)	$527 per ton
Fresh olivine makeup	$249 per ton
Hydrotreating catalyst	$20 lb^{-1}
SMR catalyst	$8 per ton hydrogen
Zinc oxide catalyst	$6 lb^{-1}
LO-CAT chemicals	$1777 per ton
Tar reformer catalyst	$22 lb^{-1}
FT catalyst	$32 lb^{-1}
Boiler chemicals	$5558 per ton
Cooling tower chemicals	$3331 per ton
Cooling tower makeup	$0.3 per ton
Waste disposal	$47 per ton
Wastewater treatment chemicals	$0.7 per ton
Wax	$0.4 lb^{-1}
Gasoline	$2.8 per gal
Diesel	$3.2 per gal
Hydrogen	$1.3 kg^{-1}

Industrial Inorganic Chemical Index from SRI Consulting,[46] and the labor indices provided by the U.S. Department of Labor Bureau of Labor Statistics.[47]

Hydrogen is a co-product and the hydrogen co-product credit is based on the hydrogen price of $2 kg^{-1} for the baseline.[48] This high hydrogen price would result in low MFSPs, so a sensitivity analysis has been performed for hydrogen prices ranging from $0.5 to $3 kg^{-1}.

Most capital expenses are sized from process simulation with base cost sourced from previous reports and models,[42,43,49] with a few exceptions specifically for the GBtL models in this paper. For instance, we use a scaling factor of 0.6 to estimate the gasifier cost with the gasifier quotation from the NREL gasification design report[42] for an inlet biomass flow higher than 2000 metric tons per day. To cater to smaller gasifier capital costs, we assume a fixed capital cost of $14MM based on a 200 dry metric tons per day biomass gasifier price,[50] with a scaling factor of 0.6.

After the total capital investment, variable operating costs, and fixed operating costs are determined, a discounted cash flow rate of return analysis has been used to determine the MFSP. The discounted cash flow analysis is calculated by iterating the selling cost of the product until the net present value of the project is zero with a 10% Internal Rate of Return (IRR). The analysis requires that the discount rate, depreciation method, income tax rates, plant life, and construction startup duration be specified. The discounted cash flow assumes 40% equity financing with a loan interest at 8% for 10 years. Working capital is assumed to be 5% of the fixed capital investment. The plant is assumed to take three years to construct plus 6 months spent toward startup.

This GBtL TEA provides baseline cost results comparable to the other evaluated biojet fuel routes and could be viewed as a near-term deployment opportunity for biojet fuel pro-

duction. According to Hicks and Tacina, fuels produced from the FT process offer advantages as compared to conventional jet fuel, including an increased thermal-oxidative stability and lower particulate emission.[60,61] More importantly, parameters or process-related variables such as material price, capital cost, operating conditions, and several processing conditions are scrutinized in the sensitivity analysis. Sensitivity analyses are performed to understand the impact of variations in the biomass-to-NG blending ratios, plant scales, design assumptions, and NG prices on the overall process economics.

A single-point sensitivity analysis is performed on the Aspen Plus model to identify key cost drivers from the selected variables. Reasonable minima and maxima for each variable with all other factors held constant are chosen to understand and quantify the resulting cost impact on overall MFSP. If the correlation is not linear, additional points might be analyzed to represent the cost impact, such as the curve for plant capacity. For example, the total production capacity changes from 10 to 100 MMGGE on an NG blending ratio range of 10% to 90%. An NG blending ratio of 10% means 10 wt% of NG is co-fed with 90 wt% of cellulosic biomass to Area 100. The total amount of feedstock is determined by the production capacity. The single-point sensitivity analysis is typically illustrated in a tornado chart with the variable impacting cost the most on the top and the variable impacting cost the least sequenced to the bottom. The single-point sensitivity analysis and scenarios analysis are focused on a single aspect while keeping all other parameters constant. However, it could be possible that several parameters are changed simultaneously so that the results would be changed significantly.

3. Process design

The goal for the baseline TEA model is to perform the sensitivity analyses to understand the impact of variations in the biomass-to-NG ratios, plant scales, reaction kinetics, process design assumptions, and NG prices on the process economics.

The process design for GBtL consists of feed handling, drying, indirect gasification, gas clean-up and conditioning, FT liquid fuel synthesis, and fractionation of liquid hydrocarbons. The NG is mixed with the biomass-derived syngas and the mixed syngas is then sent to the tar reforming area where the molar ratio of H_2/CO is adjusted to 2.1 to meet targets for the FT process. After the tar reforming process, the syngas is quenched and the acid gas (e.g., H_2S and CO_2) is removed from the syngas. Then the conditioned syngas is sent for FT synthesis to hydrocarbon fuels. The description for each area is shown in Table 3, with details in the following sections. The detailed process flow diagrams (shown in Fig. 1) and an Aspen Plus model have been developed, and material and energy flows have been evaluated. Aspects about energy integration and process design (e.g., process equipment and estimation of operating costs) and complete economic evaluation of the GBtL integrated process have been studied. In this

Table 3 Brief descriptions for each processing area

Area	Description
Area 100: preprocessing	Biomass feedstock is handled, stored, and dried.
Area 200: gasification	Biomass is gasified using indirect gasification.
Area 300: conditioning	The mole ratio of H_2/CO is adjusted to 2.1 using tar reforming and gas conditioning, including CO_2 scrubber and sulfur removal.
Area 400: FT synthesis	The adjusted syngas is converted to hydrocarbon fuels with wax as a residual product.
Area 500: product separation	Gasoline, jet, diesel, wax, and light gases are separated.
Area 600: utilities	Heat and power are co-generated to supply to the facility; n-site wastewater treatment facility.
Area 700: cooling water	Cooling tower is used to reject waste heat to the atmosphere.

study, we selected a blending ratio of 10% NG and a production capacity of 50 MMGGE per year (MMGY) of hydrocarbon fuels as a baseline. Different blending ratios and capacities have been studied in the sensitivity analysis section.

3.1 Biomass gasification

The indirect steam gasifiers are heated *via* heat transfer from a hot solid or through a heat transfer surface. Coproduct char and portions of the product gas can be combusted with air (external to the gasifier itself) to provide the energy for gasification. In this study, indirect steam gasification is chosen as the basis for the gasifier design, because previous NREL studies[42,62] have shown that it has an economic advantage over oxygen-blown high-temperature slagging gasification[62] or lower temperature dry-ash direct gasification[63] processes for the scale typical of biomass gasification. The primary reaction in indirect gasification is the devolatilization of biomass to gases, condensable vapors, and char as reaction products.[64] Feedstock composition, gasifier type, residence time, operating parameters (*e.g.*, temperature and pressure), and the relative importance of gas-phase reactions such as water gas shift[9,64] would affect the final gas composition of the gasifier. The choice of the gasification reactor influences the composition of syngas considerably, as shown in Table 4.

Table 4 Typical gas composition of raw syngas from gasification[9]

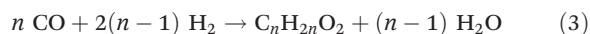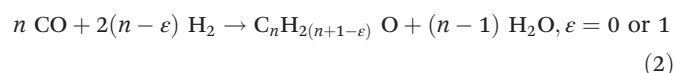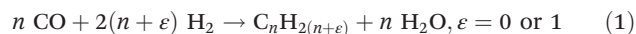| Compound	Oxygen gasification (entrained flow)	Oxygen gasification (fluidized bed)	Steam gasification (indirect)
CO (vol%)	40–60	20–30	20–25
CO_2 (vol%)	10–15	25–40	20–25
H_2 (vol%)	15–20	20–30	30–45
CH_4 (vol%)	0–1	5–10	6–12
N_2 (vol%)	0–1	0–1	0–1
LHV (MJ m^{-3})	10–12	10–12	10–14
Tar content (g Nm^{-3})	<0.1	1–20	1–10

3.2 Gas conditioning

The conditioning area contains three sub-areas, which are steam reforming, acid gas removal, and sulfur removal. For the tar reforming area, the NG is fed directly to the reformer with the biomass-derived syngas. The reformer operates at 1650 °F (900 °C) and 27 psia. Among the reforming reactions, the SMR reaction is: $H_2O + CH_4 \rightarrow CO + 3H_2$ coupled with the water–gas shift reaction: $H_2O + CO \rightarrow CO_2 + H_2$. After the reforming process, the ratio of H_2/CO in the syngas is adjusted to 2.1 by controlling the steam used in the steam reforming process. The conversion of CH_4 is assumed to be 80%. There is a 3 psia pressure drop across the reformer. The catalysts for tar reforming are priced at \$21.63 lb^{-1} and have a density of 92.5 lb ft^{-3}. The GHSV of the tar reformer reactor is 2476 h^{-1}. The reforming reaction is supported by a fuel combustor, which provides energy for the reformer.
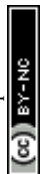
After the reforming area, the compressed fresh syngas (430 psia per 30 bar) enters an amine-based acid gas removal (AGR) unit for removal of the 82% of CO_2 and 94% of H_2S and subsequently enters the FT synthesis reactor. The recovered H_2S-rich acid gas stream is routed to the Merichem LO-CAT sulfur recovery unit. The acid gases removed in the amine scrubber are stripped to regenerate the sorbent and sent through a sulfur removal operation using a liquid phase oxidation process. The AGR and LO-CAT processes work together to remove most of the sulfur and CO_2 to the levels (*i.e.*, sulfur free and $CO_2 \leq 5\%$) desired for the copper/zinc oxide/alumina catalyst.[51]

3.3 Fischer–Tropsch synthesis

The FT process involves the catalytic conversion of syngas into a mixture of reaction products that could be refined to synthetic fuels, lubricants, and petrochemicals.[65] One of the important advantages that the FT process offers is its capability to produce liquid hydrocarbon fuels from syngas, which are almost free from sulfur and possess fewer aromatics than gasoline, jet fuel, and diesel fuel.[66] An important aspect of this process is the adjustment of the H_2-to-CO ratio, which is usually determined by the upstream gasification and reforming technologies employed.[67] As described by de Klerk,[65] the FT reaction involves catalytic CO polymerization and hydrogenation, where the chain growth and termination of the reaction products can be described by a carbon number distribution. The generic stoichiometry for the FT reactions could be described by the following chemical reactions (eqn (1)–(3)):

$$n\ CO + 2(n + \varepsilon)\ H_2 \rightarrow C_nH_{2(n+\varepsilon)} + n\ H_2O, \varepsilon = 0\ or\ 1 \quad (1)$$

$$n\ CO + 2(n - \varepsilon)\ H_2 \rightarrow C_nH_{2(n+1-\varepsilon)}O + (n - 1)\ H_2O, \varepsilon = 0\ or\ 1 \quad (2)$$

$$n\ CO + 2(n - 1)\ H_2 \rightarrow C_nH_{2n}O_2 + (n - 1)\ H_2O \quad (3)$$

The H_2/CO ratio plays an essential role in the FT process. Cobalt-based catalysts have a low water gas shift activity, which implies that syngas should have an H_2/CO ratio of 2.15 to ensure high conversion as suggested by Dry.[11] Furthermore,

for iron-based catalysts possessing a higher water gas shift reaction activity, operating temperature plays a major role. At 446 °F (230 °C) low-temperature Fischer–Tropsch (LTFT), a H_2/CO ratio of 1.7 has been recommended to ensure high conversion. Another possibility exists to conduct the reaction at 446 °F (340 °C) high-temperature FT where the water gas shift reaction proceeds rapidly to equilibrium and CO_2 can also be converted into reaction products.[11] As the FT reaction is significantly exothermic, an essential requirement is to remove heat rapidly so as to avoid temperature rise resulting in the formation of CH_4 and leading to catalyst deactivation (sintering and coking) and disintegration (due to Boudouard carbon deposition).[11]

A cobalt-based slurry column reactor is chosen and alternative catalyst and reactor configurations can be accounted for in the sensitivity analysis. The carbon number distribution in an FT process is typically described by the Anderson Schulz Flory (ASF) distribution, which essentially describes the molar concentration (x_n) of a carbon chain with n carbons in terms of a chain growth probability (α), such that the carbon numbers (n) and molar concentrations (x_n) have a logarithmic relationship[65] (eqn (4)).

$$\ln(x_n) = n \ln(\alpha) + \ln((1-\alpha)/\alpha) \qquad (4)$$

For this TEA, we chose the FT reaction at LTFT (446 °F/ 230 °C) using a cobalt-based slurry column reactor. The FT kinetics chosen to maximize the production of hydrocarbon fuel is calculated using the ASF distribution. A stoichiometric reactor model was formulated in Aspen Plus using the product yields determined on a mass basis by the ASF distribution for $\alpha = 0.84$.

3.4 Process integration

In this model, the heat and power are integrated in the steam area. The system includes a steam cycle that produces steam through the integrated recovery of heat from the hot process streams throughout the plant. Power for plant operations is produced from the steam cycle using a two-stage steam turbine with intermediate reheat to increase electricity production. The steam turbine efficiencies are assumed as 75% and the generator mechanical efficiencies are assumed to be 97%.[42,43] The plant energy balance is controlled by the rate of syngas combustion in the regenerator for the tar reformer catalyst. The energy from syngas combustion is recovered from the flue gas and contributes to the conversion to electricity in steam turbine generators.

The recycled water from the GBtL system is fed as the boiler feed water. Then water is heated in the boiler to produce the steam. Operations requiring steam include gasification, reforming, and acid gas removal sections. Steam is directly injected into the gasifier and the reformer. For the remaining hot streams that need to be cooled down, the cooling water is used to reduce the temperature to meet the temperature requirement. The cooling water is sourced from the blowdown water in the steam area and the makeup cooling water. A

mechanical draft cooling tower provides cooling water to several heat exchangers in the plant. The cooling tower uses fans to force the air through circulated water.

In the GBtL Aspen Plus model considered in this study, the recycled syngas is split into two streams. One stream is sent to the fuel combustor to generate the heat and meet the energy balance requirement for the GBtL process. The other stream is sent to the tar reformer for improving the efficiency of the reforming process. The split of the recycled syngas process is modeled by a splitter that requires a specific split ratio, which represents the portion of recycled syngas that is sent to the tar reformer. This syngas split ratio has a significant effect on the carbon efficiency as well as energy integration, and could be used to synthesize the hydrocarbon fuels. However, the option of combusting the syngas and generating the electricity from the steam generation area exists. There is a trade-off between the MFSP of the hydrocarbon fuels and sale of electricity, which may result in significant effect on the final MFSP. The syngas split ratio is a sensitive parameter for the MFSP and its effect has been studied in the section on sensitivity analysis.

3.5 Greenhouse gas life cycle assessment

LCA on GHG emissions is performed to evaluate and compare GHG emissions associated with hydrocarbon blendstock produced from the GBtL. It is wise to conduct LCA early in the design stages and throughout research and development. LCA enables the researchers to implement changes to modify and improve the sustainability of the entire life cycle, resulting in a more environmentally friendly product or process than otherwise might be produced.

A complete LCA typically will evaluate multiple impact categories, including global warming potential, acidification, eutrophication, resource depletion, and water use. While LCA can certainly be employed to evaluate a wide range of sustainability indicators, this study focuses only on global warming potential as it will help determine the maximum amount of natural gas that can be co-processed and still meet the Renewable Fuel Standard (RFS) GHG emission targets for advanced biofuels (i.e., a 50% reduction from petroleum fuel).

The scope of the LCA study concentrates on WTW life cycle GHG emissions represented in grams of carbon dioxide equivalent (CO_{2e}) using a 100-year GHG emission factor.[68] The system boundaries for the LCA analysis are shown in Fig. 2. LCA includes all the stages of a product's life—from the extraction of raw materials through the materials' processing, manu-

Fig. 2 Life cycle stages considered in the GBtL pathway.

facturing, distribution, use, and disposal or recycling. For this analysis, we account for all the stages in the life cycle of the hydrocarbon fuel, including feedstock production and logistics, fuel production and transportation, and fuel consumption. The functional unit is 1 megajoule (MJ) of fuel consumed (*i.e.*, WTW).

The LCA model is developed with SimaPro v.8.0.2 software,[69] which is used to develop and link units quantifying life cycle impacts. GHG basis values for biomass feedstock production and logistics, fuel transportation and end use, electricity, hydrogen, and NG are applied consistently with the values utilized in Argonne National Laboratory's GREET model software.[70] The Ecoinvent v.2.2 database[71] and the U.S. Life Cycle Inventory[72] processes are used to fill the data gaps. It is assumed that carbon sequestered during growth of biomass ends up in the fuel production step and returns to the atmosphere in the exhaust stream after the fuel combusts in the engine and is treated as credit. The material and energy flows for the GBtL conversion step capture the impacts of input raw materials, and outputs, such as emissions, wastes, and coproducts as predicted by the process model. The coproducts (excess electricity, wax, hydrogen, and sulfur) are treated as avoided products using the product displacement method.[73] Coproduct displacement (also termed system boundary expansion) is based on the concept of displacing the existing product with the new product.

4. Results and discussion

4.1 Baseline TEA results

The plant scale is designed for an annual production of 50 MMGGE hydrocarbon fuels. If the blending ratio between biomass and NG is roughly 90% to 10%, it requires 1684 dry metric tons per day woody biomass and 194 metric tons per day NG. The ratio of H_2/CO of the syngas from the biomass gasification is less than 2.1 : 1.0. If the gasification produces H_2/CO at a ratio much less than 2.1, a reformer is used to produce H_2 and bring the ratio up for FT synthesis.

For the baseline, the NG is charged to the tar reformer with biomass-derived syngas. The syngas ratio could be adjusted by using water gas shift in the tar reforming reactions. A small portion of the H_2 from syngas is separated by an on-site pressure swing adsorption (PSA) unit to supply to the hydrotreater. When the biomass to NG ratio is 90% : 10% (referred to as the 90/10 baseline in the following text), no excess hydrogen is made. When more NG is blended in, then there is excess hydrogen generation (for 90% NG blending, 70% NG blending, and 50% NG blending cases).

If more NG is blended, the stoichiometric ratio of NG reforming is 3, which results in a relative excess of hydrogen based on the analyzed cases. Therefore, increasing the amount of syngas from the NG reforming process could increase the H_2/CO ratio. Since an H_2/CO ratio of 2.1 is required for FT synthesis, excess hydrogen could be produced. The effect of the amount of blended NG on yield and hydrocarbon production

Table 5 Feedstock flows (dry metric tons per day) for different blending ratio of NG and biomass for annual production of 50 MMGGE hydrocarbon fuels

NG blending ratio (with remaining % from biomass)	100%	90%	70%	50%	10%	0%
Biomass (metric tons per day)	—	108	349	640	1684	2359
NG (metric tons per day)	1060	975	815	640	194	—

cost is an important aspect in design of a GBtL process, which is analyzed through sensitivity analyses. The designs for different NG and biomass blending ratios are shown in Table 5, all using an annual production of 50 MMGGE hydrocarbon fuel.

4.1.1 Yield and production. Table 6 shows the hydrocarbon yield distribution for the 90/10 baseline, with a total fuel production of 50 MMGGE per year. LHVs of all the gasoline- and diesel-range hydrocarbon fuels are converted to a GGE basis. The diesel fuel (categorized by C_{12} to C_{22} *n*-paraffins), gasoline fuel (categorized by C_5 to C_{11} *n*-paraffins), and wax (categorized by C_{23} *n*-paraffins and above) are listed separately in Table 6.

The energy efficiency is calculated on both higher heating value (HHV) and LHV. The carbon efficiency is around 35.5% independent of whether NG is reformed by itself or along with syngas from biomass gasification. For a 100% biomass case, the carbon efficiency is 29%, which is in the range of 23%–41%, presented in Table 6. The yield and efficiency values are similar to literature data of gasoline, diesel, and wax shown in Table 7. Efficiencies ranging from 30% to 50% based on chemical energy (η_{HS}) and 25%–45% based on carbon recovered through hydrocarbon products (η_{carbon}) have been reported in the literature for the BtL process.[74] Major factors that influence carbon efficiency are:

• Minimization of oxygen consumption in gasification so that carbon loss to CO_2 can be minimized.

• Improvement in hydrocarbon selectivity during FT synthesis by optimizing the reaction conditions.

• Inclusion of hydrocracking to reduce carbon to make wax.

• Exploring conceptual process strategies that allow for the addition of H_2 in the process (either as the addition of CH_4 for gasification reaction, or H_2 to FT synthesis).

Table 6 Summary of hydrocarbon fuel yields and cost for 90/10 baseline case

Diesel fuel (MMGGE per year)	31.2
Gasoline fuel (MMGGE per year)	19.4
Wax (MMGGE per year)	5.9
Total fuel production (MMGGE per year)[a]	50.6
GGE per ton dry biomass	70.2
GGE per ton NG	103.3
Gasifier LHV energy efficiency	72.6%
Plant LHV energy efficiency	69.8%
Carbon efficiency	35.5%

[a] Wax is a coproduct and is not included in the GGE calculation.

Table 7 Yield and efficiency values (carbon or heating value ratio of liquid hydrocarbon products and biomass feedstock) from FT process studies[74]

	Tijmensen et al.[66]	Dimmig et al.[75]	Schaub[76]	Leible et al.[77]
Feed flow dry (tons per h)	80	100	100	20–25
Feed flow dry (GW)	0.37	0.5	0.5	20–25
Product flow				30–45
Gasoline (tons per h)			6–7	6–12
Diesel (tons per h)			9–10	0–1
Total hydrocarbon (tons per h)	10–15	18	15–17	10–14
η_{carbon}[a] %	23–41	36	34	23–27
η_{HS}[b] %	32–51	45	42	29–34

[a] η_{carbon} is defined as the ratio of the mass of carbon (m_C) in C_5–C_{20} to the mass of carbon (m_C) in biomass feed. [b] η_{HS} is defined as the conversion efficiency based on the HHV. It is defined as the ratio of HHV of C_5–C_{20} to the HHV of the biomass feed.

4.1.2 Operating cost. Raw materials costs include feedstock (biomass and NG), chemicals (e.g., boiler chemicals, cooling tower chemicals, ammonia, and catalysts), and waste disposal. All of the unit costs for materials are listed in Table 2 in 2011 U.S. dollars. The biomass feedstock price has been considered as $80 per dry short ton, contributing $1.0 per GGE. NG is another raw feedstock, which contributes to $0.34 per GGE. NG price is considered as $238.80 per ton, equivalent to $5 per MMBTU in 2011$.[78]

The total hydrocarbon fuels production costs using GGE as a basis is shown in Table 8, with electricity and wax as coproducts. A portion of the electricity generated is used to power the facility, while the remaining electricity is sold to the grid as a coproduct. For the purpose of optimizing the overall process economics, the excess electricity is minimized in the process modeling, while maintaining energy integration of the entire facility.

4.1.3 Capital cost. Previous NREL studies have been utilized for sizing the equipment and for calculating capital costs, which are based on vendor quotes and literature.[42,43] Table 9 shows the capital cost distribution of each section for both processes. The baseline FT reactor is designed at 446 °F (230 °C) LTFT using a cobalt-based slurry column reactor. The FT synthesis system has the largest cost contribution of 47% of the total capital cost. The gas conditioning and gasification areas play an important role and constitute 21% of the total capital cost. The utility area also constitutes 11% of the total capital cost, indicating that heat integration is critical to this thermochemical pathway. The Lang Factor is 4.0, which includes all the equipment cost, additional installation and indirect costs. The total capital investment is $570 MM for a

Table 8 OPEX distribution for all hydrocarbons (C_5–C_{23}) for 90/10 base case, per GGE basis

Parameters	Cost ($ per GGE)
Feedstock	$0.98
NG	$0.34
Other raw materials	$0.12
Waste disposal	$0.01
Electricity	($0.14)
Wax	($0.40)
Total OPEX	$0.90

Table 9 Capital cost for GBtL for hydrocarbon fuel production for 90/10 base case in 2011$ (MM)

Installed costs	Cost
Gasification	$57
Gas conditioning	$69
FT synthesis	$155
Product separation	$5
Cooling water	$4
Utilities (combined heat and power)	$37
Total installed cost	$327
Total indirect cost	$203
Fixed capital investment	$541
Total capital investment	$570

facility with an annual production of 50 MMGGE hydrocarbon fuels.

4.1.4 Minimum fuel selling price. Using a 10% IRR and discounted case flow methodologies, MFSP can be estimated similar to previous TEA approaches.[79,80] The total production cost of gasoline- and diesel-range fuel production from GBtL includes variable operating costs, fixed operating costs (labor, supplies, and overhead), capital depreciation, average income tax, and average return on investment. The plant capacity is 50 MMGGE per year, which has an input of 1684 dry metric tons woody biomass and the imported NG is calculated as 194 metric tons per day (10% NG co-feeding with 90% biomass). Fig. 3 and
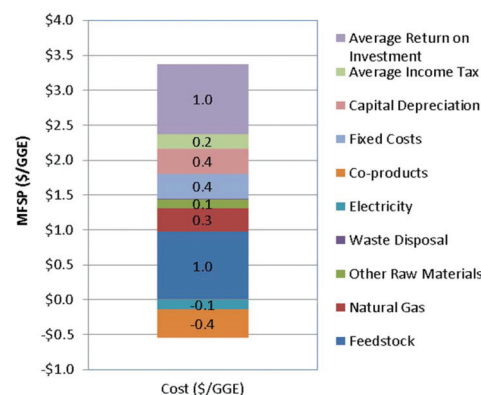
Fig. 3 MFSP cost distribution for 90/10 base case in GGE basis.

Table 10 MFSP distribution (2011$) for 90/10 base case in GGE basis

| Parameters	$ per GGE
Total OPEX	$0.9
Fixed costs	$0.4
Capital depreciation	$0.4
Average income tax	$0.2
Average return on investment	$1.0
MFSP	**$2.99**

Table 10 show the MFSP. The hydrocarbons (C_5 to C_{23}) are converted to GGE using the LHV. The coproducts considered are electricity and wax, and hydrogen in some cases. As indicated in Fig. 3, the average return on investment, NG, and feedstock costs are the most important positive operating costs. The MFSP is calculated based on the LHV of the produced hydrocarbons using diesel fuel and GGE basis. The MFSP is $2.99 per GGE for the GBtL baseline (90% biomass and 10% NG). Table 10 shows the MFSP distributions on a GGE basis.

4.2 Sensitivity analysis results

For single-point sensitivity analysis, several critical parameters are explored, including variations of selected key parameters. The difference of scenario analysis and single-point sensitivity analysis is that several processing parameters have been adjusted with each α value while in single-point sensitivity analysis; all other process parameters are kept unchanged.

4.2.1 Tornado chart. Fig. 4–6 show the sensitivity analyses for 50 MMGY capacity cases whose NG blending ratios are 10%, 50%, and 90%, respectively. These three cases are selected to see the impacts of the sensitivity parameters on the final MFSP for a facility with different NG blending ratios. The selection of 90%, 10%, and 50% NG is intended to reflect high, middle, and low points on a blending curve, so that different ranges of NG blending ratios could be investigated. The mass flows of both NG and biomass for these three cases are given in Table 11, all targeting to produce 50 MMGY of hydrocarbon fuels. The selected sensitivity parameters are plant scale, biomass price, total capital cost, syngas split ratio to syngas *versus* combustor, FT synthesis reactor capital cost,
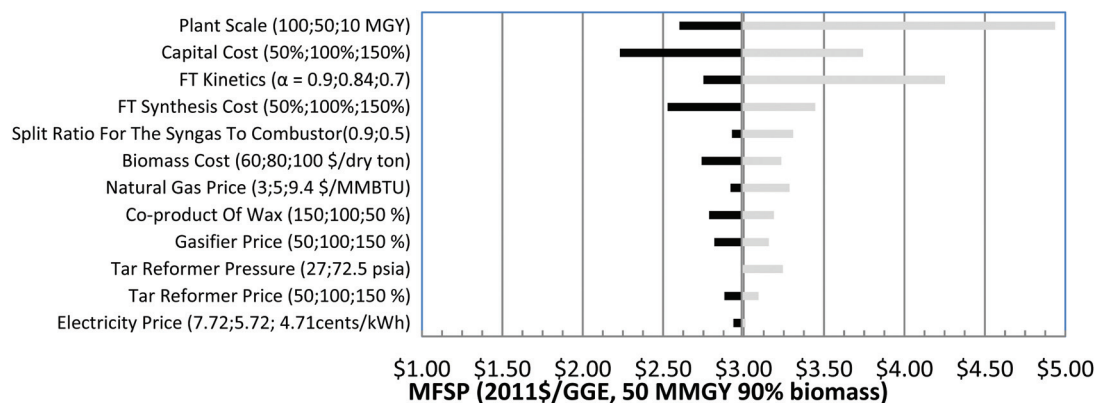
Fig. 4 Tornado chart for 10% NG and 90% biomass GBtL process with annual 50 MMGY hydrocarbon fuels.
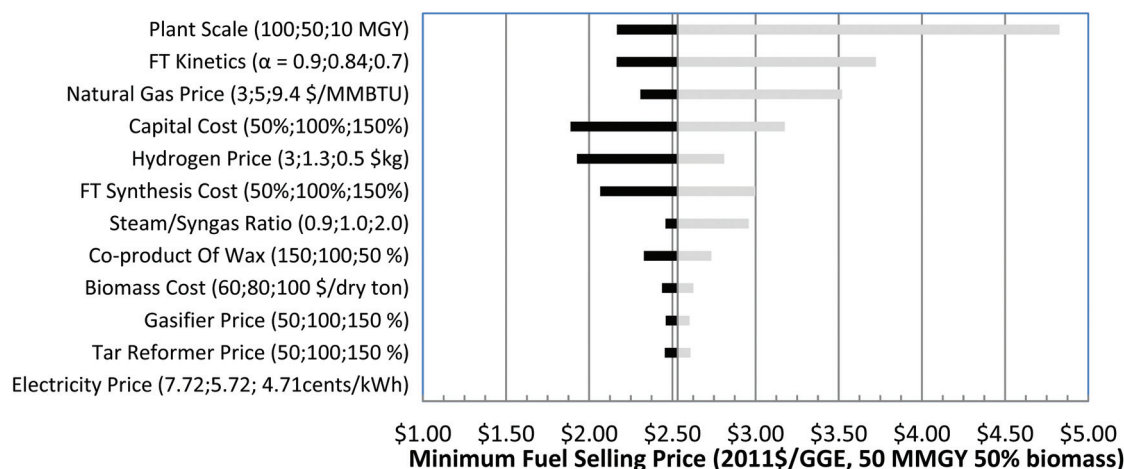
Fig. 5 Tornado chart for 50% NG and 50% biomass GBtL process with annual 50 MMGY hydrocarbons.
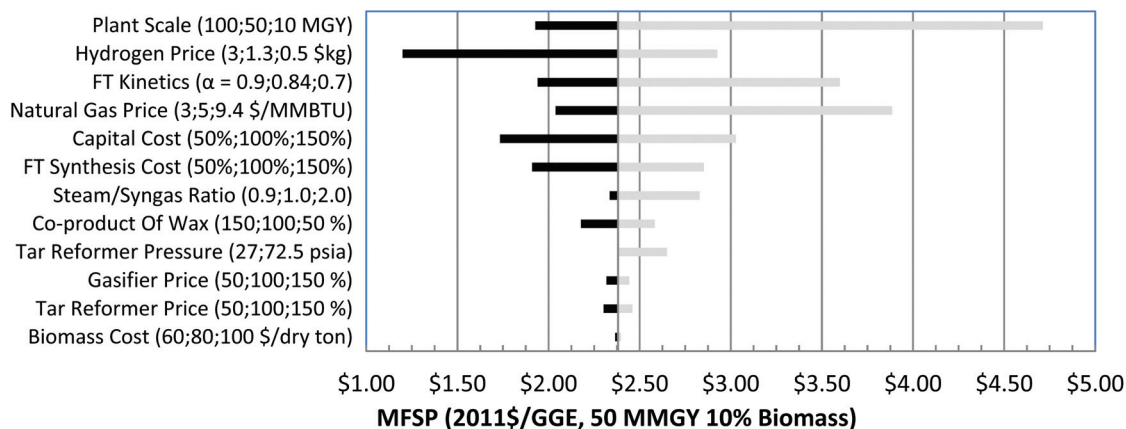
Fig. 6 Tornado chart for 90% NG and 10% biomass GBtL process with annual production of 50 MMGY hydrocarbons.

Table 11 TEA results for different NG blending ratios (at capacity of 50 MMGY)

Blending NG % (remaining percentage from woody biomass)	100% of NG	90% of NG	70% of NG	50% of NG	10% of NG	0% NG
Biomass (metric tons per day)	—	108	349	640	1684	2359
NG (metric tons per day)	949	975	815	640	194	—
MFSP ($ per GGE)	2.22	2.38	2.43	2.53	2.99	3.28
Carbon efficiency (wt%)	50.13%	45.3%	45.1%	44.2%	35.5%	29.7%
Fixed capital investment ($MM)	461	463	453	461	541	618
GGE per ton biomass	—	89.5	89.2	87.3	70.2	58.6
GGE per ton NG	145.36	131.7	131.3	128.5	103.3	—
Gal per dry ton biomass	—	90.5	90.1	88.3	70.9	59.2

gasifier capital cost, tar reformer capital cost and pressure, and electricity, wax, NG, and hydrogen prices for all three blending ratios.

The syngas split ratio represents the portion of recycled. Syngas that is sent to the tar reformer. It is a significant parameter for the GBtL system since it affects the yield of CO and H_2 and the hydrocarbon fuel production capacity and cost. The tar reformer pressure could affect the heat requirement of the tar reformer and influence the heat balance of the GBtL system. The plant scale ranges from 10 to 100 MMGY. The gasifier cost, tar reformer cost, FT synthesis area cost, wax coproduct credit, and the total capital cost is varied in the range of 50%–150% of the baseline.

NG price range is defined from EIA data to be $3–$9.40 per MMBTU.[78] The electricity price range is based on the history of the minimum and maximum average retail monthly electricity price during 2001 to 2015 from EIA[81] to be 4.71–7.72 cents per kWh. For some cases, when co-feeding a high percentage of hydrogen-rich NG, there is excess hydrogen production for coproduct revenue. The hydrogen price is assumed to be $1.29 kg^{-1} for the baseline and ranges from $0.50 to $3 kg^{-1}.

Fig. 4 shows the sensitivity analyses for 10% NG in the 50 MMGY capacity case, with calculated MFSP from $2.23 to $4.94 per GGE. Capital cost is second only to plant scale, influencing cost significantly. MFSP could be as high as $3.74 per GGE when the capital cost is increased to 150% of the baseline

capital cost. Higher α values also favor cost reduction. FT kinetics are the third most important parameter, which results in a range of $2.75–$4.25 per GGE of MFSP. Among all the process areas, the FT synthesis area constitutes the largest portion of the total capital cost, and hence the FT reactor contributes to capital cost significantly. Because the blended NG is only 10% of total feedstock, the mass flow of NG is 194 metric tons per day, which is much lower than mass flow of biomass at 1684 metric tons per day. As a result, the NG price has a smaller effect on the MFSP than biomass cost.

In summary, plant scale is always the most important factor for all three analyses in varying the blending ratio of NG and biomass. Other factors like capital cost, raw materials, and coproduct prices are the major cost drivers. Along with the change of blending ratio of NG and biomass, the order of importance for the parameters changes accordingly. The more NG that is blended in, the more important its cost. The key cost drivers are blending ratios of NG, optimization of heat integration of the process, and the reduction of excess hydrogen and electricity production.

4.2.2 Plant scale and blending ratio of NG and biomass. In Table 11, variations of the blending ratio between biomass and NG are studied for carbon efficiency and capital cost, with a targeted plant scale of 50 MMGY. The carbon efficiency for the GBtL process is improved from 29% to 45% if the weight percentage of NG blended is increased from 0% to 100%, so
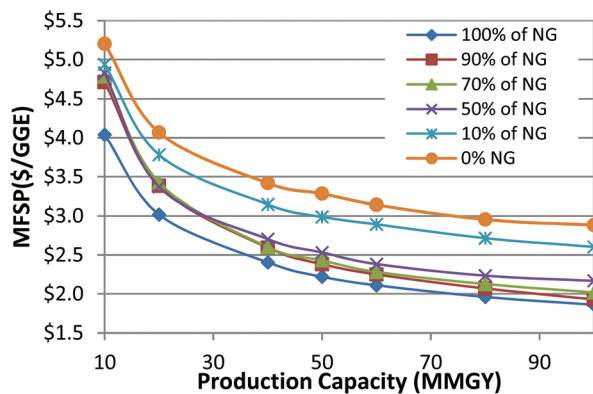
Fig. 7 The effect of both plant scales and NG and biomass blending ratios on MFSP.

hydrocarbon production increases. Also, the capital cost is decreased along with increasing of the NG blending ratio because the capital cost of gasifiers is reduced if comparatively less amount of biomass is used. Fig. 7 shows the effect of both plant scale (from 10 to 100 MMGY) and blending ratios of NG and biomass (0% to 100% mass flow of NG).

There are a few important insights that have been identified by studying the variation of the blending ratio of NG and biomass feedstocks. First, the MFSP decreases with the increase of production capacity, due to economies of scale. Second, when the NG blending ratio is less than 50%, the ratio of H_2/CO for the syngas used for FT synthesis is lower than the targeted 2.1 for FT synthesis, which requires the water gas shift reaction in the reforming step to increase the amount of hydrogen. As a result, there is no excess hydrogen produced. When the NG blending ratio is higher or equal to 50%, the ratio of H_2/CO for the syngas would be higher than 2.1, so water–gas shift is no longer needed. A PSA unit is employed to split a portion of the hydrogen from the syngas. The excess hydrogen split from the PSA unit is sold as the coproduct.

The co-feeding of biomass along with NG offers the advantage of the economies of scale associated with NG. For instance, if the cost target is $3 per GGE, the plant capacity has to be more than 70 MMGY for BtL (0% NG curve shown in Fig. 7). However, approaching the same cost target, the plant capacity could be reduced to 50 MMGY with the blending of 10% NG and 90% biomass. The plant capacity could be further reduced to 20 MMGY if using 100% NG as feedstocks. This is not only because NG has a higher heating value per weight, but also because blending NG with cellulosic materials could increase the total hydrocarbon yields. Co-feeding of biomass with NG would simultaneously reduce the carbon dioxide emissions of NG by integrating it with a renewable feedstock. Additional investigation on LCA on various blending ratios of biomass and NG is discussed in the life cycle assessment results section.

4.2.3. Energy integration and its impacts to cost of liquid fuels. Unconverted syngas is recycled and split into two

streams. One stream is sent to the fuel combustor to generate the heat for the whole GBtL energy demand (heating and power), while the other stream is recycled to the tar reformer to improve total carbon efficiency of feedstocks. In the Aspen Plus model, the split of the recycled syngas is modeled by a splitter with a specific split ratio. This specified split ratio represents the portion of recycled syngas that is sent to the tar reformer. It is a significant parameter for the GBtL system since it affects the yield of CO and H_2, hydrocarbon fuel production, and ultimately cost. Ideally, only sufficient syngas should be sent to the combustor so that the hydrocarbon production would be maximized if more syngas is sent to the tar reformer. On the other hand, the electricity production for the GBtL system would be enhanced if more syngas is sent to the combustor for heat generation. More electricity production means lower hydrocarbon yield, resulting in higher MFSP, even if excess electricity is sold to the grid as a coproduct.

Fig. 8 shows the effect of the syngas split ratio on MFSP and MMGY using 90% biomass and 10% NG. The split ratio ranges from 0.5 to 0.9 are studied. As indicated in Fig. 8, the MFSP is linearly reduced from $3.3 per GGE to $2.9 per GGE if the split ratio increases from 0.5 to 0.9 at an electricity selling price of 5.72 cents per kWh.[81] This is due to hydrocarbon production that is linearly increased from 38.5 to 53 MMGY. As also highlighted in the figure, the impact of this syngas split ratio varies when assuming different electricity prices.

The trend of MFSP based on the 4.71 cents per kWh case has a sharper slope than that based on the 7.72 cents per kWh case. When the electricity price is high enough, the effect of the syngas split ratio on the MFSP is minimized due to an improved value obtained with the sale of electricity.

4.2.4 Tar reformer pressure. The tar reformer pressure is another important factor that influences the MFSP. Fig. 9 shows the effect of tar reforming pressure on the MFSP for the 10% NG blending ratio (at a capacity of 50 MMGY hydrocarbon fuel production), assuming pressure changing from 30 to 72.5 psia. The resulting MFSP increases from $2.99 to $3.24 per GGE, due to incremental cost in constructing thicker reactors to meet pressure ratings. Aspen Economic Analyzer is used to detect the relationship between pressure rating and equipment cost for the tar reformer. It is found that the equip-
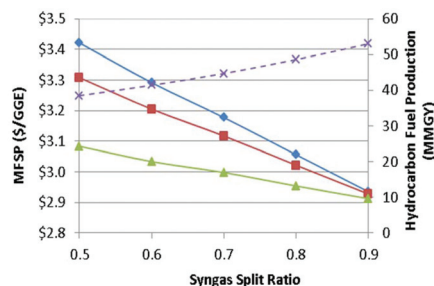
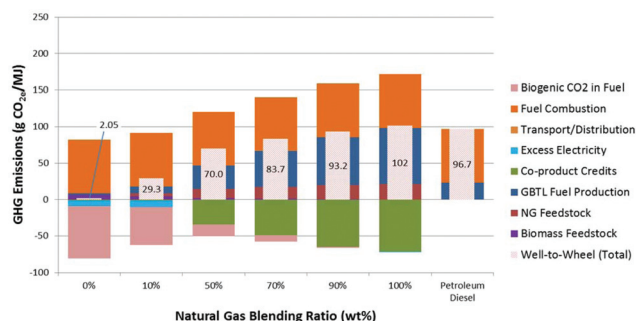**Fig. 8** The effect of syngas split ratio on MFSP and MMGY using 90% biomass and 10% NG.

Fig. 9 Life cycle GHG emissions of hydrocarbon blendstock *via* GBtL as a function of NG blending ratio.

Fig. 10 MFSP and life cycle GHG emissions for hydrocarbon blendstock produced *via* GBtL as a function of NG blending ratio, assuming annual production of 50 MMGY hydrocarbon fuels.

ment cost increases linearly with the pressure rating, from eqn (5):

$$\text{Equipment cost ($MM)} = 0.1934 \times \text{pressure (psia)} + 0.8361. \tag{5}$$

4.3 Life cycle assessment results

The projected WTW GHG emissions for a compression–ignition, direct injection vehicle using hydrocarbon fuel produced *via* the GBtL as a function of the NG blending ratio is shown in Fig. 9. The stacked bar depicts the contribution from each life cycle stage. The WTW GHGs increases with increasing NG blending ratio, ranging from 2.05 g CO_{2e} per MJ (0% NG) to 102 g CO_{2e} per MJ (100% NG). Stages that contributed the most are the fuel production and fuel combustion. It is noteworthy that GHGs for the fuel combustion stage for all cases are identical at 73.5 g CO_{2e} per MJ (same vehicle); however, biogenic CO_2 (from fuel originated from biomass) in the fuel combustion emission is credited, and consequently the net GHGs for the fuel combustion stage is directly proportional to the NG blending ratio. For the 0% and 100% NG blending cases, the fuel is derived entirely from the biomass and NG, respectively; all the fuel combustion CO_2 emissions are biogenic CO_2 for the former and fossil CO_2 for the later.

Coproduct credits are only associated with the conversion stage. As a design constraint, the process was designed without the need to purchase electricity or fossil fuel for plant operations. For the cases that result in excess heat or power production, energy in the form of electricity will be exported to the grid for a coproduct credit. The electricity coproduct credits for the 0% and 10% NG cases are 7.1 and 8.3 g CO_{2e} per MJ, respectively. Excess electricity diminishes at a higher NG blending ratio, partly due to lower production of biochar that is used for heat and power generation.

As the biofuel industry develops, TEA coupled with LCA will play a key role in process development and targeting of technical and economic barriers for the emerging conversion pathways. As exhibited in Fig. 10, co-processing NG readily offers an economic advantage predominantly due to factors such as higher NG conversion efficiency, lower capital cost (smaller gasifier), and richer hydrogen content in the feedstock.
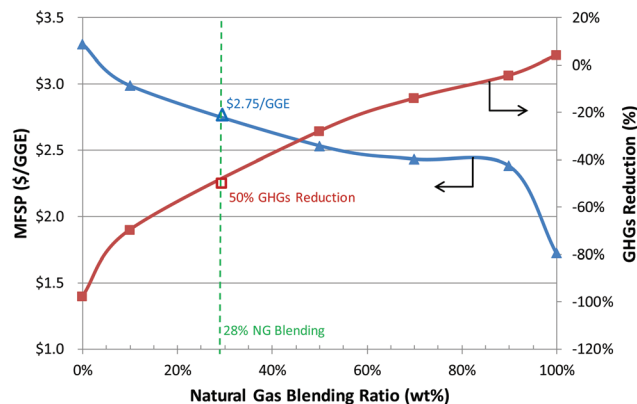
The improved MFSP is at the expense of environmental sustainability, namely higher fossil GHG emissions. The life cycle GHGs increase with increasing the NG blending ratio. Without any NG co-processing (0% NG case), the life cycle GHGs were estimated to be 2.05 g CO_{2e} per MJ, corresponding to a 98% GHG reduction relative to the 2005 petroleum diesel baseline GHGs (96.7 g CO_{2e} per MJ).[82] The WTW GHGs for the 100% NG blending case are 102 g CO_{2e} per MJ and are similar to the GREET result for the NG-to-diesel *via* FT pathway at 104 g CO_{2e} per MJ.[70] Below 90% NG blending ratio, NG co-processing exhibits life cycle WTW GHGs less than that from petroleum diesel.

It is also determined that the current GBtL pathway can readily co-process up to 28% NG and still meet the GHG threshold reduction target for the advanced biofuels set by the U.S. Environmental Protection Agency (EPA).[83] At 28% NG blending, the corresponding WTW GHG reduction and MFSP are 50% and $2.75 per GGE, respectively.

While not included in this study, the WTW GHG emissions can potentially be further mitigated by implementing carbon management practices at the biorefinery, such as carbon capture and sequestration technologies. Other alternatives including co-processing renewable biogas instead of pipeline NG can also improve the carbon footprint. These approaches will lead to higher allowable NG blending ratio that will enable the GBtL technology by displaying both economic and environmental sustainability.

5. Conclusion

Detailed GBtL economic and environmental analyses were performed using a blended feedstock consisting of woody biomass and NG. The integrated process includes biomass gasification to syngas, NG steam reforming to syngas, and conversion of syngas to hydrocarbon blendstocks through FT. Consistent with other TEA efforts, a biomass feedstock cost of $80 per dry ton, NG price of $5 per MMBTU, and 90% overall

process efficiency was considered with 2011 as the cost year basis. When co-feeding 10% NG with 90% biomass, the MFSP for this baseline model predicts $2.99 per GGE considering hydrocarbon fuel production (22 MM gallons of jet fuel, 19 MM gallons of naphtha, and 9 MM gallons of diesel), with annual total hydrocarbon production of 50 MMGGE. Sensitivity analyses were performed to understand the impact of variations in the biomass-to-natural-gas ratio, plant scales, design assumptions and NG prices on the economics and the design of the GBtL process. Key findings from this analysis are described below.

At a NG price of $5 per MMBTU, the MFSP from this GBtL process is reduced by co-feeding NG. As the blending ratio of NG to biomass increases, the MFSP decreases. However, the LCA study reveals that less than 30% (by weight) of NG can be blended to meet a 50% GHG emission reduction threshold, shown in Fig. 10. The key cost drivers are blending ratios of NG, optimization of heat integration of the process, and the reduction of excess hydrogen and excess electricity production. The addition of methane from NG helps to overcome the low amount of H_2 in biomass, to bring the H_2/CO ratio closer to the desired $2.1:1$. Thus, when combining both NG and biomass to product hydrocarbon liquid fuels, carbon efficiency of the hydrocarbon fuels is improved.

The co-feeding of biomass along with NG also offers the advantage of the economies of scale associated with either biomass or NG, while simultaneously reducing the carbon dioxide emissions of NG by integrating it with a renewable feedstock. If the goal is to achieve the same cost target, a higher blending ratio of NG will result in a facility with smaller production capacity. The GBtL process provides better economies of scale with higher NG blending ratios (see Fig. 10). Other more advanced and recently developed syngas-to-olefins, syngas-to-mixed-oxygenates, or syngas-to-mixed-alcohols pathway technologies could be considered as process alternatives for future studies, which will help in providing a greater understanding of GBtL.

LCA results reveal that co-processing NG enables the economic feasibility of converting biomass to the liquid fuel but at the expense of environmental sustainability. The life cycle GHG emissions increase with increasing co-fed NG. To meet the 50% life cycle GHG reduction threshold for advanced biofuels set by the EPA, the maximum NG blending ratio is determined to be about 28%, corresponding with the favorable MFSP of $2.75 per GGE. Achieving even lower MFSP requires co-processing NG higher than 28% without violating the GHG reduction requirement, and this can potentially be accomplished by implementing carbon management practices at the biorefinery and or co-processing renewable biogas instead of pipeline NG.

Abbreviations

AGR	Acid gas removal
ASF	Anderson Schulz Flory
bbl	Barrel
BtL	Biomass-to-liquid
BTU	British thermal unit
CO_{2e}	Carbon dioxide equivalent
CtL	Coal-to-liquid
EIA	U.S. Energy Information Administration
EPA	U.S. Environmental Protection Agency
FT	Fischer–Tropsch
GBtL	Natural gas and biomass-to-liquid
GGE	Gallon gasoline equivalent
GHG	Greenhouse gas
GtL	Gas-to-liquid
HHV	Higher heating value
IRR	Internal rate of return
kBD	Thousand barrels per day
LCA	Life cycle assessment
LHV	Lower heating value
LTFT	Low-temperature Fischer–Tropsch
MFSP	Minimum fuel selling price, cost based on the sum of all the hydrocarbons using gallon gasoline equivalent basis
MJ	Megajoule
MM	Million
MMGY	Million gallon gasoline equivalent per year
NG	Natural gas
NREL	National Renewable Energy Laboratory
OPEX	Operating expense
OT-CCS	Once-through with CO_2 capture
OT-V	Once-through with CO_2 venting
PSA	Pressure swing adsorption
R&D	Research and development
RFS	Renewable Fuel Standard
scfpd	Standard cubic feet per day
SMR	Steam methane reformer
TEA	Techno-economic analysis
U.S.	United States
WTW	Well-to-wheel

Conflicts of interest

There are no conflicts to declare.

Acknowledgements

process disclosed, or represents that its use would not infringe privately owned rights. Author E. C. D. T. contributed the LCA study. We appreciate all the editing help from our technical editors, Justin A. Rickard, Kathy L. Cisar and Billie Christen.

Notes and references

1 U.S. Energy Information Administration, *International Energy Outlook 2014: World Petroleum and Other Liquid Fuels*, Report DOE/EIA-0484(2014), 2014.

2 Bioenergy Technolgies Office, *The Potential for Natural Gas to Enhance Biomass Technologies*, 2014.

3 U.S. Department of Energy, *EERE/BETO, Growing America's Energy Future*, 2013.

4 A. Dutta, J. Hensley, R. Bain, K. Magrini, E. C. D. Tan, G. Apanel, D. Barton, P. Groenendijk, D. Ferrari, W. Jablonski and D. Carpenter, Technoeconomic Analysis for the Production of Mixed Alcohols via Indirect Gasification of Biomass Based on Demonstration Experiments, *Ind. Eng. Chem. Res.*, 2014, **53**, 12149–12159.

5 A. H. Lillebø, A. Holmen, B. C. Enger and E. A. Blekkan, Fischer–Tropsch conversion of biomass-derived synthesis gas to liquid fuels, *Wiley Interdiscip. Rev.: Energy Environ.*, 2013, **2**, 507–524.

6 N. E. T. Laboratory (NETL), *Analysis of Natural Gas-to Liquid Transportation Fuels via Fischer-Tropsch*, Report DOE/NETL-2013/1597, U.S. Department of Energy, Office of Fossil Energy, 2013.

7 N. E. T. L. (NETL), *Baseline Technical and Economic Assessment of a Commercial Scale Fischer–Tropsch Liquids Facility*, Report DOE-NETL-2007/1260, 2007.

8 H. A. Wright, J. D. Allison, D. S. Jack, G. H. Lewis and S. R. Landis, ConocoPhillips GTL Technology: The COPox™ Process as the SynGas Generator, *Prepr. Pap.-Am. Chem. Soc., Div. Fuel Chem.*, 2003, **48**, 791–792.

9 R. Rauch, J. Hrbek and H. Hofbauer, Biomass gasification for synthesis gas production and applications of the syngas, *Wiley Interdiscip. Rev.: Energy Environ.*, 2014, **3**, 343–362.

10 C. Higman and S. Tam, Advances in Coal Gasification, Hydrogenation, and Gas Treating for the Production of Chemicals and Fuels, *Chem. Rev.*, 2014, **114**, 1673–1708.

11 M. E. Dry, High quality diesel via the Fischer–Tropsch process – a review, *J. Chem. Technol. Biotechnol.*, 2002, **77**, 43–50.

12 A. M. Saib, D. J. Moodley, I. M. Ciobîcă, M. M. Hauman, B. H. Sigwebela, C. J. Weststrate, J. W. Niemantsverdriet and J. van de Loosdrecht, Fundamental understanding of deactivation and regeneration of cobalt Fischer–Tropsch synthesis catalysts, *Catal. Today*, 2010, **154**, 271–282.

13 Shell News, Pearl GTL – an overview, http://www.shell.com/global/aboutshell/major-projects-2/pearl/overview.html.

14 R. C. Baliban, J. A. Elia and C. A. Floudas, Biomass to liquid transportation fuels (BTL) systems: Process synthesis and global optimization framework, *Energy Environ. Sci.*, 2013, **6**, 267–287.

15 R. C. Baliban, J. A. Elia, C. A. Floudas, B. Gurau, M. B. Weingarten and S. D. Klotz, Hardwood biomass to gasoline, diesel, and jet fuel: 1. Process synthesis and global optimization of a thermochemical refinery, *Energy Fuels*, 2013, **27**, 4302–4324.

16 G. Haarlemmer, G. Boissonnet, E. Peduzzi and P.-A. Setier, Investment and production costs of synthetic fuels – A literature survey, *Energy*, 2014, **66**, 667–676.

17 USDoE, Coal and Biomass to Liquids, http://energy.gov/fe/coal-and-biomass-liquids, accessed May 19, 2015.

18 A. M. Niziolek, O. Onel, J. A. Elia, R. C. Baliban, X. Xiao and C. A. Floudas, Coal and biomass to liquid transportation fuels: Process synthesis and global optimization strategies, *Ind. Eng. Chem. Res.*, 2014, **53**, 17002–17025.

19 R. C. Baliban, J. A. Elia, V. Weekman and C. A. Floudas, Process synthesis of hybrid coal, biomass, and natural gas to liquids via Fischer-Tropsch synthesis, ZSM-5 catalytic conversion, methanol synthesis, methanol-to-gasoline, and methanolto-olefins/distillate technologies, *Comput. Chem. Eng.*, 2012, **47**, 29–56.

20 J. A. Elia, R. C. Baliban and C. A. Floudas, Toward novel hybrid biomass, coal, and natural gas processes for satisfying current transportation fuel demands, 2: Simultaneous heat and power integration, *Ind. Eng. Chem. Res.*, 2010, **49**, 7371–7388.

21 R. C. Baliban, J. A. Elia and C. A. Floudas, Optimization framework for the simultaneous process synthesis, heat and power integration of a thermochemical hybrid biomass, coal, and natural gas facility, *Comput. Chem. Eng.*, 2011, **35**, 1647–1690.

22 R. C. Baliban, J. A. Elia and C. A. Floudas, Simultaneous process synthesis, heat, power, and water integration of thermochemical hybrid biomass, coal, and natural gas facilities, *Comput. Chem. Eng.*, 2012, **37**, 297–327.

23 Z. Haq and P. Gupte, The Potential for Natural Gas to Enhance Biomass Technologies: Technical Barriers and Greenhouse Gas Emissions/Resource Potential, http://energy.gov/sites/prod/files/2014/04/f14/february2014_gbtl_webinar.pdf, accessed May 18, 2015.

24 Y. Dong and M. Steinberg, Hynol - An economical process for methanol production from biomass and natural gas with reduced CO2 emission, *Int. J. Hydrogen Energy*, 1997, **22**, 971–977.

25 R. H. Borgwardt, Biomass and natural gas as co-feedstocks for production of fuel for fuel-cell vehicles, *Biomass Bioenergy*, 1997, **12**, 333–345.

26 I. S. Ermolaev, V. S. Ermolaev and V. Z. Mordkovich, Efficiency of gas-to-liquids technology with different synthesis gas production methods, *Ind. Eng. Chem. Res.*, 2014, **53**, 2758–2763.

27 A. de Klerk, in *Fischer-Tropsch Refining*, Wiley-VCH Verlag GmbH & Co. KGaA, 2011, pp. 73–103, DOI: 10.1002/9783527635603.ch4.

28 P. M. Maitlis and A. de Klerk, *Greener Fischer-Tropsch Processes for Fuels and Feedstocks*, John Wiley & Sons, 2013.

29 E. C. University, GTL Technology and Its Role in the World Energy Markets (online), http://www.eni.com/en_IT/attachments/lavoraconnoi/pdf/GTL-technology.pdf.

30 D. A. Wood, C. Nwaoha and B. F. Towler, Gas-to-liquids (GTL): A review of an industry offering several routes for monetizing natural gas, *J. Nat. Gas Sci. Eng.*, 2012, **9**, 196–208.

31 E. D. Attanasi and P. A. Freeman, *Role of stranded gas in increasing global gas supplies*, Report 2013–1044, U.S. Geological Survey Open-File Report, 2013.

32 R. C. Baliban, J. A. Elia and C. A. Floudas, Biomass and natural gas to liquid transportation fuels: Process synthesis, global optimization, and topology analysis, *Ind. Eng. Chem. Res.*, 2013, **52**, 3381–3406.

33 O. Onel, A. M. Niziolek, J. A. Elia, R. C. Baliban and C. A. Floudas, Biomass and natural gas to liquid transportation fuels and olefins (BGTL+C2-C4): Process synthesis and global optimization, *Ind. Eng. Chem. Res.*, 2015, **54**, 359–385.

34 A. M. Niziolek, O. Onel, J. A. Elia, R. C. Baliban and C. A. Floudas, Coproduction of liquid transportation fuels and C6_C8 aromatics from biomass and natural gas, *AIChE J.*, 2015, **61**, 831–856.

35 T. Fleisch, *Associated Gas Monetization via miniGTL Conversion of flared gas into liquid fuels & chemicals*, Global Gas Flaring Reduction Partnership, The World Bank, 2014.

36 S. Chakravarti, D. P. Bonaquist, R. F. Drnevich and M. M. Shah, Natural gas enhanced biomass to liquids: Project development and modeling, *Comput. Chem. Eng.*, 2012, **47**, 67–75.

37 S. Chakravarti, R. F. Drnevich, D. P. Bonaquist and G. Panuccio, Using fossil fuels to increase biomass-based fuel benefits, Google Patents, 2013.

38 R. C. Baliban, J. A. Elia and C. A. Floudas, Biomass and Natural Gas to Liquid Transportation Fuels: Process Synthesis, Global Optimization, and Topology Analysis, *Ind. Eng. Chem. Res.*, 2013, **52**, 3381–3406.

39 O. Onel, A. M. Niziolek, J. A. Elia, R. C. Baliban and C. A. Floudas, Biomass and natural gas to liquid transportation fuels and olefins (BGTL+C2_C4): process synthesis and global optimization, *Ind. Eng. Chem. Res.*, 2015, **54**, 359–385.

40 G. Liu, R. H. Williams, E. D. Larson and T. G. Kreutz, Design/economics of low-carbon power generation from natural gas and biomass with synthetic fuels co-production, *Energy Procedia*, 2011, **4**, 1989–1996.

41 M. M. Wright, N. Seifkar, W. H. Green and Y. Román-Leshkov, Natural Gas and Cellulosic Biomass: A Clean Fuel Combination? Determining the Natural Gas Blending Wall in Biofuel Production, *Environ. Sci. Technol.*, 2015, **49**, 8183–8192.

42 A. Dutta, M. Talmadge, J. Hensley, M. Worley, D. Dudgeon, D. Barton, P. Groenendijk, D. Ferrari, B. Stears, E. M. Searcy, C. T. Wright and J. R. Hess, *Process Design and Economics for Conversion of Lignocellulosic Biomass to Ethanol, Thermaochemical Pathway by Indirect Gasification and Mixed Alcohol Synthesis*, Report NREL/TP-5100-51400, National Renewable Energy Laboratory, 2011.

43 R. Davis, *Techno-economic analysis of current technology for Fischer-Tropsch fuels production (EPA Technical Memorandum)*, 2009.

44 *AspenPlus^{TM}, Release 7.2*, Aspen Technology Inc., Cambridge MA, 2007.

45 *Chemical Engineering Magazine*, Chemical Engineering Magazine Plant Cost Index, 2011.

46 SRI Consulting, *Chemical Economics Handbook*, 2008.

47 Bureau of Labor Statistics Data website, National Employment, Hours, and Earnings Catalog, Industry: Chemicals and Allied Products, 1980–2009.

48 K. Randolph, Hydrogen Production-2013 Annual Merit Review and Peer Evaluation Meeting, 2013.

49 H2A Production Model, Version 3., http://www.hydrogen.energy.gov/h2a_production.html.

50 H. Knoef, *Handbook Biomass Gasification*, BTG biomass technology group, 2005.

51 E. Tan, M. Talmadge, A. Dutta, J. Hensley, J. Schaidle, M. Biddy, D. Humbird, L. J. Snowden-Swan, J. Ross, D. Sexton, R. Yap and J. Lukas, *Process Design and Economics for the Conversion of Lignocellulosic Biomass to Hydrocarbons via Indirect Liquefaction*, 2015.

52 U. S. Energy Information Administration, U.S. Natural Gas Prices, http://www.eia.gov/dnav/ng/ng_pri_sum_dcu_nus_a.htm, accessed July 2013.

53 U. S. EIA, Electricity Retail Price to Consumers, http://www.eia.gov/electricity/data.cfm#sales, accessed July 2013.

54 A. Dutta, A. Sahir, E. Tan, D. Humbird, L. J. Snowden-Swan, P. Meyer, J. Ross, D. Sexton, R. Yap and J. Lukas, *Process Design and Economics for the Conversion of Lignocellulosic Biomass to Hydrocarbon Fuels Thermochemical Research Pathways with In Situ and Ex Situ Upgrading of Fast Pyrolysis Vapors*, Report NREL/TP-5100-62455, National Renewable Energy Laboratory, 2015.

55 Syntroleum, Syntroleum Analyst Day, http://library.corporate-ir.net/library/83/834/83417/items/201092/AnalystDay_June2006.pdf.

56 ICIS, Paraffin wax US prices, markets & analysis, https://www.icis.com/chemicals/paraffin-wax/us/, 2013.

57 U. S. Energy Information Administration, Petroleum and other Liquid, *Refiner Gasoline Prices by Grade and Sales Type*, https://www.eia.gov/dnav/pet/pet_pri_refoth_dcu_nus_m.htm, accessed in 2012.

58 U. S. Energy Information Administration, Weekly Retail Gasoline and Diesel Prices, http://www.eia.gov/dnav/pet/pet_pri_gnd_dcus_nus_a.htm, 2014.

59 B. Suresh, R. Gubler, X. He and Y. Yamaguchi, *Chemical Economics Handbook Hydrogen (743.5000)*, IHS, 2015.

60 Y. R. Hicks and K. M. Tacina, *Spring Technical Meeting of the Central States Section of the Combustion Institute April 22–24, 2012, Comparing a Fischer-Tropsch Alternate Fuel to*

JP-8 and their 50-50 Blend: Flow and Flame Visualization Results.

61 J. Klettlinger, R. Rich and C. Yen, *Energytech, 2011 IEEE, Thermal Stability Testing of Fischer-Tropsch Fuel and Various Blends With Jet A, as well as Aromatic Blend Additives*, 2012.

62 A. Dutta, R. L. Bain and M. J. Biddy, Techno-economics of the production of mixed alcohols from lignocellulosic biomass via high-temperature gasification, *Environ. Prog. Sustainable Energy*, 2010, **29**, 163–174.

63 A. Dutta and S. Phillips, *Thermochemical ethanol via direct gasification and mixed alcohol synthesis of lignocellulosic biomass*, National Renewable Energy Laboratory Golden, CO, 2009.

64 R. L. Bain, K. A. Magrini-Bair, J. Hensley, W. S. Jablonski, K. M. Smith, K. R. Gaston and M. M. Yung, Pilot Scale Production of Mixed Alcohols from wood, *Ind. Eng. Chem. Res.*, 2014, **53**, 2204–2218.

65 A. de Klerk, in *Kirk-Othmer Encyclopedia of Chemical Technology*, 2013, DOI: 10.1002/0471238961.fiscdekl.a01.

66 M. J. A. Tijmensen, A. P. C. Faaij, C. N. Hamelinck and M. R. M. van Hardeveld, Exploration of the possibilities for production of Fischer Tropsch liquids and power via biomass gasification, *Biomass Bioenergy*, 2002, **23**, 129–152.

67 A. d. Klerk, Fischer-Tropsch fuels refinery design, *Energy Environ. Sci.*, 2011, **4**, 1177–1205.

68 S. Solomon, D. Qin, M. Manning, Z. Chen, M. Marquis, K. B. Averyt and H. L. Miller, *Contribution of Working Groups I to the Fourth Assessment Report of the Intergovernmental Panel on Climate Change: Physical Science Basis*, Report 0961-9534, Cambridge University Press, New York, USA, 2007.

69 *SimaPro, v8.2.2*, Product Ecology Consultants, Amersfoort, the Netherlands, 2016.

70 GREET2, *The Greenhouse Gases, Regulated Emissions, and Energy use in Transportation (GREET) model, in rev1*, Argonne National Laboratory, 2012.

71 Ecoinvent, *Ecoinvent, v.2.2; Swiss*, Center for Life Cycle Inventories, Duebendorf, Switzerland, 2010.

72 LCI, *U.S. Life-Cycle Inventory, v.1.6.0*, National Renewable Energy Laboratory, Golden, CO, 2008.

73 Q. Wang, J. Luo, Z. Zhong and A. Borgna, CO2 capture by solid adsorbents and their applications: Current status and new trends, *Energy Environ. Sci.*, 2011, **4**, 42–55.

74 D. Unruh, K. Pabst and G. Schaub, Fischer–Tropsch synfuels from biomass: maximizing carbon efficiency and hydrocarbon yield, *Energy Fuels*, 2010, **24**, 2634–2641.

75 T. Dimmig and M. Olschar, *Sekund€arenergietr€ager aus Biomasse, Eine systemanalytische Untersuchung*.

76 G. Schaub, D. Unruh and M. Rohde, *Biomasse-Vergasung; Der Konigsweg für eine effiziente Strom- und Kraftstoff-Bereitstellung?* Landwirtschaftsverlag GmbH, Münster, Germany, Schriftenreihe Nachwachsende Rohstoffe, 2004, vol. 24, pp. 351–362.

77 L. Leible, S. K€alber, G. Kappler, S. Lange, E. Nieke and P. Pro plesch, *Kraftstoff, Strom und W€arme aus Stroh und Wald restholz;Eine systemanalytische Untersuchung, Wissenschaftliche restholz;Eine systemanalytische Untersuchung*, Wissenschaftliche ruhe, Germany, 2007.

78 U. S. Energy Information Administration, Natural Gas Prices, http://www.eia.gov/dnav/ng/ng_pri_sum_dcu_nus_a.htm, accessed in 2015.

79 R. P. Anex, A. Aden, F. K. Kazi, J. Fortman, R. M. Swanson, M. M. Wright, J. A. Satrio, R. C. Brown, D. E. Daugaard, A. Platon, G. Kothandaraman, D. D. Hsu and A. Dutta, Techno-economic comparison of biomass-to-transportation fuels via pyrolysis, gasification, and biochemical pathways, *Fuel*, 2010, **89**(suppl), S29–S35.

80 D. Humbird, R. Davis, L. Tao, C. Kinchin, D. Hsu, A. Aden, P. Schoen, J. Lukas, B. Olthof, M. Worley, D. Sexton and D. Dudgeon, *Process Design and Economics for Biochemical Conversion of Lignocellulosic Biomass to Ethanol:: Dilute-Acid Pretreatment and Enzymatic Hydrolysis of Corn Stover*, 2011.

81 U. S. Energy Information Administration, *Electricity Data Browser-Average Retail Price of Electricity*, accessed in 2015.

82 Government Printing Office, Supplemental determination for renewable fuels produced under the final RFS2 program from grain sorghum, *Fed. Regist.*, 2012, **77**, 74592–74607.

83 US-EPA, Fuels & Fuel Additives, Renewable Fuel Standard (RFS), http://www.epa.gov/otaq/fuels/renewablefuels.